Research Article

Feifei Jia, Guoling Li, Bo Yang, Bing Yu, Youqing Shen, and Hailin Cong

Investigation of rare earth upconversion fluorescent nanoparticles in biomedical field

https://doi.org/10.1515/ntrev-2019-0001
Received Nov 25, 2018; accepted Nov 27, 2018

Abstract: Rare earth upconversion nanoparticles (UCNPs) with the superior performance in the biomedical field have attracted great attention. Due to the good light stability, low toxicity, deep tissue penetration and excellent biocompatibility, UCNPs display great potential for development in the biomedical field. Excellent related reports are increasing year by year, like molecular sensing, bioimaging and therapeutics. In this paper, the preparation, modification, application of upconversion fluorescent nanoparticles and the latest research results in the field of biomedical materials have been reported in detail.

Keywords: rare earth upconversion nanoparticles; preparation; modification; biomedical materials

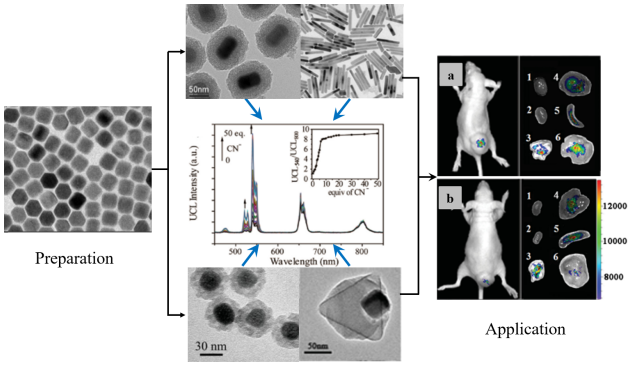

Graphical abstract: In this paper, we systematically summarize and describe the preparation, modification, application and latest discovery in biomedical field of rare earth upconversion nanoparticles (UCNP). Due to the good light stability, low toxicity, deep tissue penetration and excellent biocompatibility, UCNPs display superior performance for the development of biomedical field in cancer therapy. Our work will certainly inspire researchers in related fields to create more meaningful upconversion nanomaterials and do more contributions to human cancer treatment research.

1 Introduction

Upconversion nanoparticles (UCNPs) is a kind of functional materials that converts low-energy photons into high-energy photons, usually composed of inorganic matrices and rare earth doped ions. The doped rare earth ions can absorb low-energy long-wavelength photons and emit high-energy short-wavelength photons through multi-photon transitions, converting the infrared light into visible light. Essentially, upconversion fluorescence is a kind of anti-Stokes light [1]. UCNPs consist of three parts, activator, sensitizer and matrix material. Activator is used as the light center. Sensitizers is used to absorb energy and transfer energy to the activator ions. The matrix material generally does not participate in the transfer of energy, but acting as a fixed dopant ion and providing the appropriate crystal field for the luminescent center. For example, β-$NaGdF_4$:Yb^{3+}, Ln^{3+} (Ln = Er^{3+}, Tm^{3+}, Ho^{3+}) [2, 3], Ln^{3+} is the activator, Yb^{3+} is the sensitizer, β-$NaGdF_4$ plays the role of matrix material. Upconversion fluorescence is based on three light-emitting mechanisms: excited state absorption (ESA), energy transfer upconversion (ETU), photon avalanche (PA), cooperative energy transfer (CET) and energy migration-mediated upconversion (EMU). ESA was presented by Bloembergen [4] *et al.* in

Hailin Cong: Institute of Biomedical Materials and Engineering, College of Materials Science and Engineering, Qingdao University, Qingdao 266071, China; Laboratory for New Fiber Materials and Modern Textile, Growing Base for State Key Laboratory, College of Chemistry and Chemical Engineering, Qingdao University, Qingdao 266071, China; Email: hailincong@yahoo.com
Feifei Jia, Guoling Li: Institute of Biomedical Materials and Engineering, College of Materials Science and Engineering, Qingdao University, Qingdao 266071, China; Authors contributed equally to this paper
Bo Yang, Youqing Shen: Institute of Biomedical Materials and Engineering, College of Materials Science and Engineering, Qingdao University, Qingdao 266071, China
Bing Yu: Institute of Biomedical Materials and Engineering, College of Materials Science and Engineering, Qingdao University, Qingdao 266071, China; Laboratory for New Fiber Materials and Modern Textile, Growing Base for State Key Laboratory, College of Chemistry and Chemical Engineering, Qingdao University, Qingdao 266071, China

Open Access. © 2019 F. Jia *et al.*, published by De Gruyter. CC BY This work is licensed under the Creative Commons Attribution 4.0 License

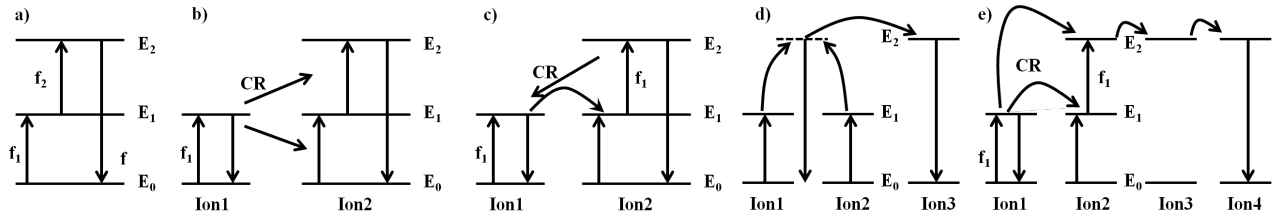

Figure 1: a) A scheme of ESA. b) A scheme of ETU. c) A scheme of PA. d) A scheme of CET. e) A scheme of EMU

1959, it means that one ion jumps from the ground state to the higher excited state through the continuous multi-photon absorption, which is shown in Figure 1a. At first, the luminescent center transfers from the ground state to the intermediate metastable E_1 by absorbing photons f_1, and then absorbs the photon energy of f_2 to reach the excited state E_2 to form two-photon absorption. Finally it returns to ground state E_0 to emit photons of frequency f. Figure 1b shows the ETU mechanism, when the energy of one ion in the excited state and the other in the ground state satisfies the energy match, the excited state ion releases energy by self-relaxation back to ground state, the other ion receives energy to a higher energy state E_2.The PA mechanism is shown in Figure 1c. Ion2 transfers from metastable E_1 to excited E_2 by absorption of f_1 and then releases part of the energy by self-relaxation back to E_1, which is transferred to Ion1 resulting the transition from E_0 to E_1. Ion1 continues back to E_0 and releases f_1 energy by self-relaxation. At this time Ion2 receives energy and transfers from E_1 to E_2 by cross-relaxation (CR), resulting in avalanche increasing. The electrons in E_2 state are unstable and back to the ground state E_0 to release more energy [5]. The biggest difference from ETU is that CET has no real intermediate energy state and is very inefficient, specifically shown in Figure 1d. In a typical CET process, two ions(Ion1, Ion2) in the middle metastable E_1 are excited to the virtual excited state E_2 and simultaneously transfer their energy to the Ion3 for upconversion. In 2011, Liu's group [6] proposed a new upconversion mechanism, energy migration-mediated upconversion (EMU) as shown Figure 1e. In this phenomenon, there are four kinds of light-emitting components, sensitizer, accumulating agent, migration agent and activator. They are integrated into different layers within nanoparticle. After laser irradiation, the EMU process occurs at the core of the nanoparticle (Ion1) and then the energy is gradually transferred from the accumulating agent(Ion2) to the migration agent(Ion3) to the activator(Ion4) to produce upconversion luminescence. These five theoretical models build the luminescence principle of UCNPs.

UCNPs are different from many organic fluorescent dyes and quantum dots (QDs), UCNPs are chemically stable and never bleach. The emission wavelengths of UCNPs do not dependent on crystal size and the multicolor emission can easily be accomplished by varying host crystal and RE dopant [7]. Organic fluorescent dyes are traditional fluorescent indicator, but the photo bleaching and photo degradation are serious because of the poor photochemical stability. In addition, the application of organic dyes is usually based on ultraviolet light or visible light as the excitation light source, whose tissue penetration is poor. Long exposure to high energy photons may lead to biomolecule damage and background fluorescence of organisms itself limit the application of organic fluorescent dyes in biomedical. Similar as fluorescent dyes, QDs also require ultraviolet light or visible light as excitation light sources, furthermore, there are biological application defects like tissue penetration, biological tissue destructiveness and autofluorescence interference. Lanthanide-doped UCNPs which can be excited by infrared irradiation can effectively solve these problems [8]. UCNPs as a new kind of functional materials have zero autofluorescence feature, rather narrow emission bands, deep tissue penetration [7, 9], tunable multicolour emission, exceptional photo stability and low toxicity in vitro or vivo [10–13]. UCNPs have been wielded applied in biological imaging, DNA detection, immunoassay, photodynamic therapy, photo catalysis, optogenetics, drug deliver and solar cells [14–17].

During recent years, UCNPs as an efficient candidate for fluorescence imaging has become a research hotspot in the field of biomedicine. In this paper, authors systemically introduce the usual preparation, modification and biomedical application of upconversion fluorescent nanoparticles. In the end, the potential of its future development in the field of biology and medicine is also prospected.

2 Preparation of upconversion nanoparticles

Controlling the synthesis of monodisperse upconverting nanoparticles is critical for the application of bioimaging and targeted therapies. Nanoparticles can be synthesized flexibly by controlling synthesis conditions including reaction temperature, reaction time, precursor concentration and surfactants, etc.There are many methods to prepare rare-earth upconversion nanoparticles, including precipitation, thermal decomposition, hydrothermal solvent heat, sol-gel method, combustion method and microemulsion method. Here, we will describe these typical synthetic lanthanide nanoparticles methods in detail.

2.1 Coprecipitation method

The precipitation method is based on precipitation reaction. Add precipitant into the salt solution containing the cationic components of the pre-prepared material, or salt solution directly hydrolysis at a certain temperature, making the ions in raw materials form various kinds of precipitations. Finally the desired product can be obtained through filtration, washing, drying and roasting decomposition. Yieta and Haase synthesized $NaYF_4$:Yb/Er (or Tm) nanoparticles by using this method. Yi *et al.* [18] and co-workers used ethylenediaminetetraacetic acid (EDTA) as a solvent to control total amount of Ln^{3+} ions and finally synthesized spherical $NaYF_4$ NPs with diameters from 37 to 166 nm. Haase *et al.* [19] creatively synthesized cubic phase $NaYF_4$:Yb/Er (or Tm) NPs with smaller size (5-30nm) by using high-boiling solvent N-(2-hydroxyethyl) ethylenediamine (HEEDA). Lu [20] synthesizes size-controlled and up-conversion luminescence-tunable Y_2O_3: Er, Yb nanoparticles by using etyltrimethylammonium bromide (CTAB) as a surfactant and adjusting green and red emission intensity of nanoparticles by controlling CTAB concentration. Representatively, Zhang [21] developed a user-friendly high temperature coprecipitation method and successfully synthesized uniform 20-30nm hexagonal phase $NaYF_4$:Yb/Er (or Tm) nanoparticles, as show Figure 2. His method can accurately control the shapes, sizes and intense upconversion luminescence (UCL). Qiu [22] creatively prepared fluorescence-enhanced Yb^{3+}/Tm^{3+}-codoped fluoride active core/active shell/inert shell nanoparticles through coprecipitation method. The precipitation method has the characteristics of simple operation process, low cost, fast nucleation growth rate and high purity of the product. However, synthetic nanoparticles often occur severe agglomeration, which is not conducive to biological applications.

2.2 Thermal decomposition method

Thermal decomposition method is based on the traditional solvent thermal method, but specifically introduce trifluoroacetic acid rare earth salt and rare earth halide that decompose at high temperatures into the reaction system. A variety of rare earth precursor salt can be prepared by adding them into high boiling organic solvents (oleic acid/carbon octadecene, oleic acid/oleyl amine, pure oil amine system). The rare earth precursors would be decomposed into rare earth fluoride nano-materials in the nitrogen atmosphere at 250~340°C.

Capobianco first reported various kinds of rare earth upconversion nanoparticles by thermal decomposition method, such as monodisperse Yb/Er or Yb/Tm co-doped $NaYF_4$NPs [23, 24], monodisperse Ln^{3+}-doped $LiYF_4$ [25, 26], $NaGdF_4$ [27] etc. Kang and co-workers [28] prepared a core–shell upconversion nanocrystals β-$NaLuF_4$:Y/Yb/Tm(Er)@$NaLuF_4$ with crystal phase and adjustable size by thermal decomposition method for dual luminescence imaging and CT in vivo. The crystal phase and size of the nanocrystals can be controlled by changing Y^{3+} concentration, and the prepared UCNPs have good monodispersity and uniform nanometer size. Feng Wang [29] reported the preparation process of $NaGdF_4$:Yb,Tm nanoparticles and core-shell $NaGdF_4$ nanoparticles doped with luminescent lanthanide ions by thermal decomposition in detail. Furthermore, they could change the size of the nanoparticles by controlling the amounts of NH_4F/methanol solutions and the obvious result is shown Figure 3. Li [30] synthesized ultrasmall β-$NaYF_4$:Yb^{3+}/Er^{3+}(10nm) core and $NaYF_4$:Yb^{3+}/Er^{3+}@$NaYF_4$ core–shell UCNPs by modified thermal decomposition. He changed the reaction temperature and the ratio of Na^+ / Ln^{3+} / F^- to control the crystal phase and particle size of the product. Different from coprecipitation method, the nanoparticles prepared by thermal decomposition method have good crystallinity, high luminous efficiency and uniform size. Furthermore, the particle size is controllable. But the reaction conditions are harsh. The whole synthesis process must be under high temperature, anhydrous and oxygen-free. The synthetic particles are usually oil-soluble and the toxicity is high.

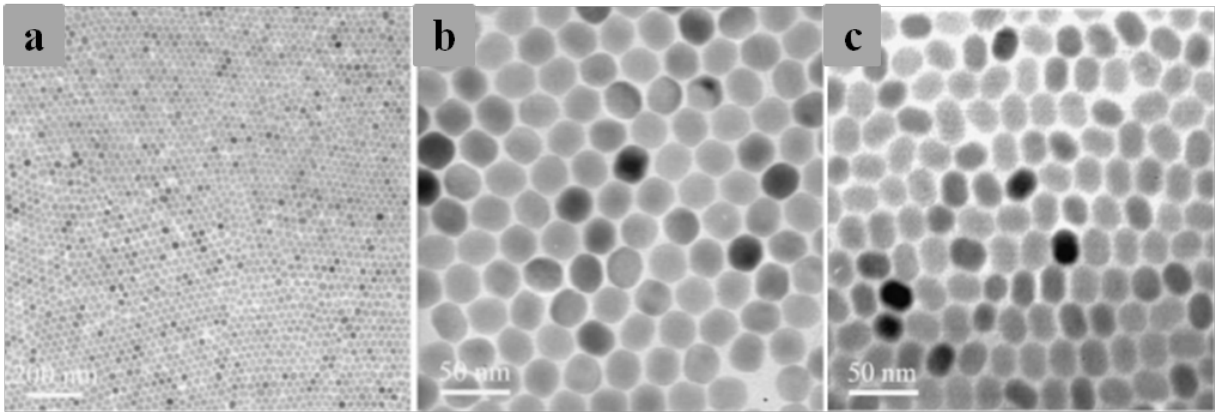

Figure 2: Control of nanocrystal shape. a–b) TEM images of $NaYF_4$:Yb, Er nanospheres at different magnifications. c) TEM images of $NaYF_4$:Yb, Er nanoellipses [21].

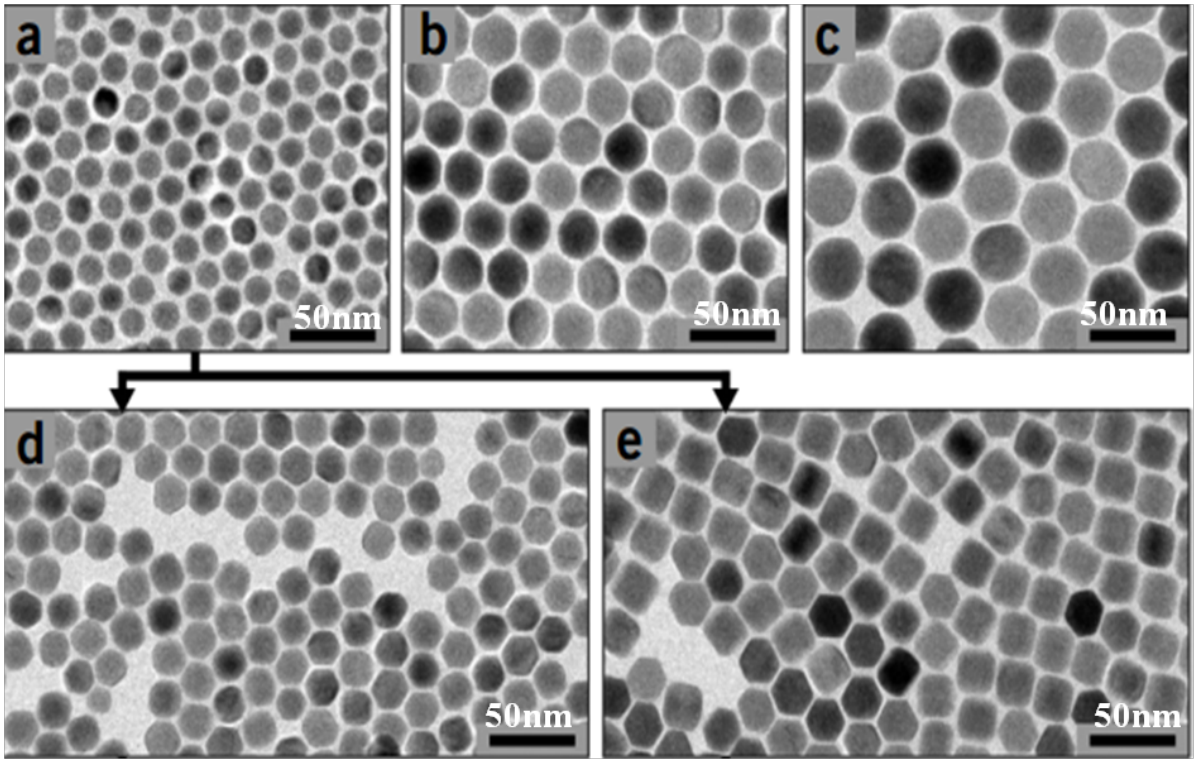

Figure 3: Size-tuning of the $NaGdF_4$ nanocrystals. a-c) TEM images of $NaGdF_4$:Yb/Tm nanocrystals prepared by adding 3.3, 3.1 and 2.7ml of NH_4F/methanol solutions, respectively. d, e) TEM images of $NaGdF_4$:Yb/Tm@$NaGdF_4$:Tb core-shell nanocrystals prepared by adding 50 and 25 mg of 15nm core particles, respectively [29].

2.3 Hydrothermal solvent thermal method

Hydrothermal solvent thermal method is generally completed in the special closed reactor under high temperature and high pressure with water or organic solvents. The reaction time, reaction temperature, ion concentration and the volume of solvent can affect the product morphology (spherical, hexagonal, nanorods, hexagonal prism etc.) and the size. The hydrothermal solvate method is simple and inexpensive, without any special high heat treatment. Liu *et al.* [11] reported preparation of Gd^{3+} doping $NaYF_4$ nanoparticles by using this method, and simultaneously controlled the crystalline phase and size etc by addition of Gd^{3+} ions. The Gd^{3+} ions promoted the phase transformation from cubic to hexagonal and reduced the particle size from large micro-tubes to small cubes, as shown in Figure 4. In addition, Wang [31] and his co-

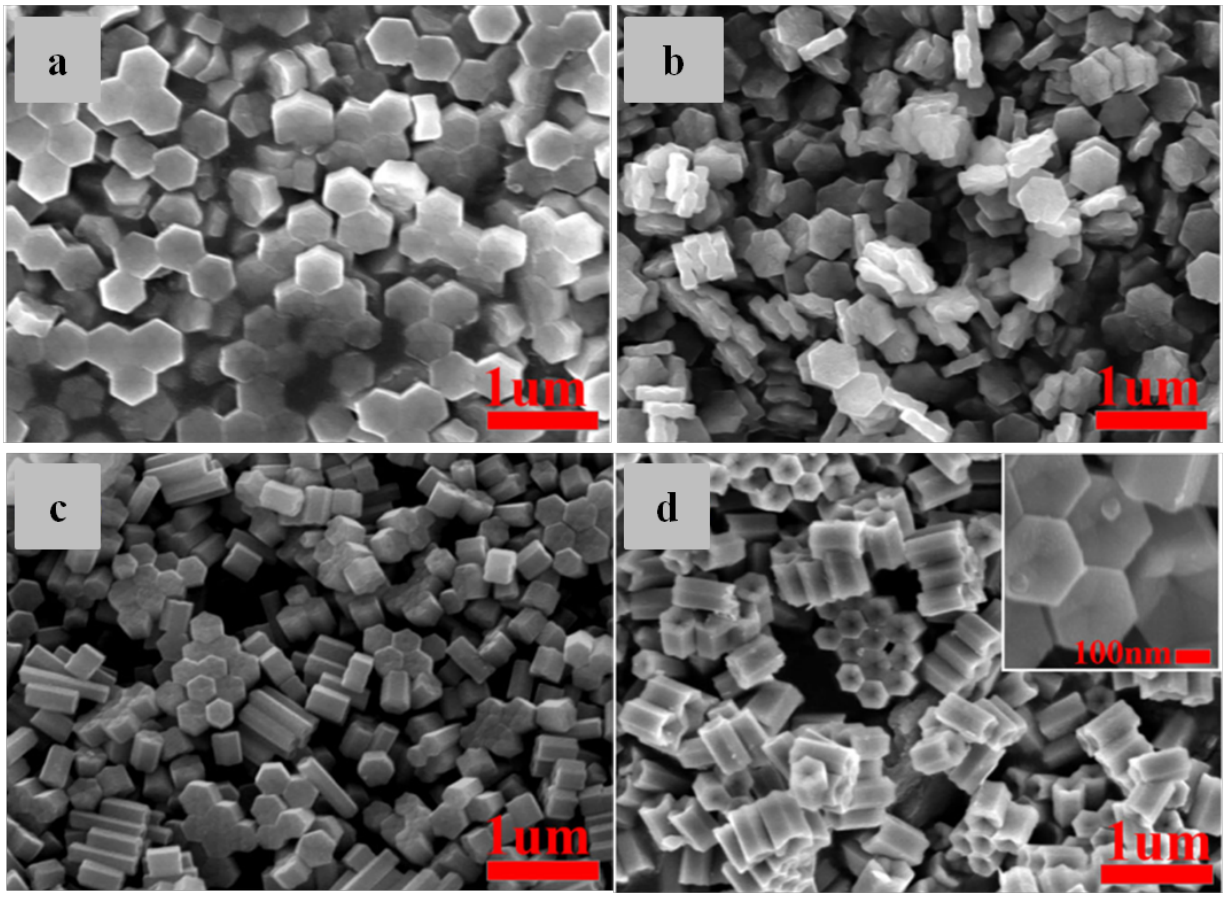

Figure 4: SEM image of the as-synthesized $NaYF_4$:Yb^{3+}/Er^{3+}/Ni^{2+} (20/2/x mol%) nanocrystals: a) x = 0, b) x = 20, c) x = 30, d) x = 40 [32].

workers also used this method to synthesize Ca doped CeF_3, Ca promoted the hexagonal cube phase transition. Recently, Yi [32] successfully synthesized Ni^{2+} ions-doped $NaYF_4$:Yb^{3+}/Er^{3+} nanoparticles by hydrothermal solvent thermal method the results show that the morphology of UCNPs changes from regular hexagons to nanorod of uniform size and size increases with ion Nd^{2+} concentration increasing, as shown Figure 4. The Hydrothermal solvent thermal method should be completed in a special closed container compared with other preparation methods, the reaction temperature is relatively low, resulting low energy consuming and high product. The size and shape of UCNPs can be well controlled. The production cost is low, which is very suitable for commercialization.

2.4 Sol-gel method

Sol-gel method refers to the method of producing various nano inorganic materials or composite materials by the solution of the organic or inorganic materials of metal through solution-sol-gel evolvement at low temperature. Sol-gel method can synthesize UCNPs with metal oxide as matrix material, including TiO:Er, $BaTiO_3$:Er, ZrO:Er [33], Lu_3Ga_5O:Er and YVO_4:Yb/Er [34]. The sol-gel method has the advantages of easy control of doping amount, low heat treatment temperature, simple equipment and low price. However, the method needs a long reaction time, the size of prepared UCNPs is difficult to control and particles are severely agglomerated after high temperature calcination, which limits the medical application.

2.5 Microemulsion method

Microemulsions are thermodynamically stable colloidal dispersions with transparent or translucent. Colloidal dispersions are usually composed of oils, water, emulsifiers and co-emulsifiers. In the microemulsion method, all chemical reactions take place inside the droplets. At the beginning of the reaction, the precipitated nuclei of the product are first formed. When the size of the particles approaches the droplet size, the film formed by the surfactant molecules adheres to the surface of the particles and

Table 1: Comparison of preparation methods of UCNPs

Method	Condition	Characteristic
Coprecipitation method	soluble salt solution, precipitant, drying roasting	simple operation process, low cost, severe agglomeration
Thermal decomposition method	high temperature anhydrous anaerobic environment	good crystallinity, high luminous efficiency, uniform size
Hydrothermal solvent thermal method	high temperature and pressure	simple, inexpensive, relatively low reaction temperature, controllable product size and shape
Sol-gel method	solution-sol-gel evolvement, low temperature	Product size is difficult to control and easy to reunite
Combustion method	explosive reaction by heating	poor product purity and luminescence
Microemulsion method	colloidal dispersions, drop reaction	poor monodispersity, low yield

acts as a "protective agent" to limit further growth of the precipitate. By using cetyltrimethylammonium bromide/2-octanol/water as microemulsion system, Shi *et al.* [35, 36] prepared CaF_2 and BaF_2 particles below 100 nm. The products prepared by the microemulsion method have poor monodispersity, and the relative yield of the prepared nanoparticles is relatively small, which is suitable for laboratory research and is difficult to be applied to large-scale production.

2.6 Combustion method

Usually, metal nitrate is mixed with organic fuel in aqueous solution and water is evaporated by heating to cause explosive reaction, and the generated large amount of heat promotes the formation of the target product. The size of the product can be controlled by varying the ratio of fuel to oxidant. Combustion method is a very meaningful and energy-efficient synthesis method in the synthesis of luminescent materials. A large number of oxide and oxysulfide UCNPs have been synthesized by this method, such as Y_2O_3, $La_2O_2S_3$ and Gd_2O_3 [37–39]. The luminescent materials synthesized by it have corresponding adaptability and the burning gas can protect the rare earth ions from being oxidized, thus eliminating the need for reducing protective atmosphere. However, the purity and luminescence properties of the products produced are not very good.

We compared the preparation methods of UCNPs and compiled a table, as shown in Table 1. Among these synthetic routes, thermal decomposition, hydrothermal solvent heat and precipitation methods are the most popular and most effective methods for preparing high quality upconverting nanoparticles, the UCNPs prepared by these methods have good monodispersity, uniform size and controllable morphology. Combustion method and microemulsion method are relatively less applied because of some inevitable disadvantages, such as severe agglomeration, poor light performance and difficult size control.

3 Functional modification of UCNPs

The monodispersed UCNPs with controlled morphology and uniform size can be obtained by a variety of methods. However, the surface of UCNPs prepared by these methods usually contains hydrophobic organic ligands such as oleic acid, oleylamine and carbon octadecene, etc. Hydrophobic UCNPs have limited their use in the biomedical applications. Therefore, the hydrophobic UCNPs must be changed into hydrophilic for biocompatible. Functionalization of UCNPs is achieved by modifying different substances on the surface of UCNPs. Surface modification methods mainly contain ligand exchange method, polymer coating method and silica coating method etc. UCNPs have inappreciable cytotoxicity and negligible organ toxicity through various modifications on the surface, showing overall safety.

3.1 Ligand exchange method

UCNPs prepared by thermal decomposition method, are covered with a layer of oleic acid molecules. Chen [40] and Wang [41] changed hydrophobic UCNPs into water-soluble by using the ligand interaction between polyacrylic acid (PAA) macromolecule and surface oleic acid molecules. Hydrophilic PAA molecules can not only convert UCNPs into water-soluble, but also the surface car-

boxyl groups can be further coupled with biomolecules. Parac-Vogt [42] prepared a novel multimodal contrast agent with biocompatibility by surface modification using PAA, showing that contrast agents doped with rare earth elements have very low cytotoxicity at 500μg/ml, no cell damage was detected. Ai [43] synthesized a highly soluble core-shell lanthanide-doped upconversion nanocrystals by using PAA for surface modification. And the carboxyl group on the PAA surface can be further coupled to biomolecules for further cellular applications. Beyerrell [44] prepared hydrophilic function UCNPs by poly (ethylene glycol) -phosphate ligands through the solvent heat pathways. Wang [45] prepared water-soluble UCNPs by surface modification using citrates. Many common organic molecules can be used as ligands to modify UCNPs, such as polyethylene glycol (PEG) [46], polyvinyl alcohol (PVA) [47], medroxyprogesterone 17-acetate (MPA) [48], polyvinylpyrrolidone (PVP) [49, 50], nitrosonium tetrafluoroborate ($NOBF_4$) [51] ect. Research shows that ligand exchange method is a simple, convenient and effective method.

3.2 Polymer coating method

UCNPs can be encapsulated by amphiphilic polymers and polyelectrolyte polymers through the layer-by-layer self-assembly method (LBL). The amphiphilic polymer coating is mainly carried on the surface of the nanoparticle by the Van der Waals force between the hydrophobic chain of polymer and the long alkyl chain of the hydrophobic UCNPs surface, finally the entire nanoparticle is water-soluble and biocompatible. Tang and coworkers [52] prepare UCNPs with stable water solubility by LBL. Positively charged polyallylamine hydrochloride (PAH) and negatively charged sodium polystyrene sulfonate (PSS) are connected to the surface of nanocrystals by LBL, and a large number of amino groups on peripheral linear polymer PAH can be further functionalized. Kim [53] *et al.* replaced the oleic acid ligand with N- (2-mercaptoethyl) carbamate tert-butyl ester with acid labile moiety that can be cleaved by UV light. As a result, the ligand is shortened and becomes more hydrophilic, also the dispersion of the particles is remarkably improved. Kamimura *et al.* [54] used negatively charged poly (ethylene glycol)-cation-poly (acrylic acid) to produce Y_2O_3 type water-dispersed UCNPs by electrostatic effect. The surface coating of UCNP can also be achieved in hydrothermal method using protective block poly (ethylene glycol) copolymer layer [55]. Chatterjee and co-worker reported the synthesis of polyethylene imine (PEI) coated UCNPs by modified hydrothermal method [56, 57]. Commonly used modified polymers are PEI [58], polypyrrole (PPY) [47], Polydopamine (PDA) [59–61], Poly (ethylene glycol)-poly (acrylic acid) diblock polymers (PEG–PAA) [62] and poly(4,5-dimethoxy-2-nitrobenzyl methacrylate) -b-poly(methoxy polyethylene glycol monomethacrylate) diblock copolymer(PNB-b-POEG) [63], as show in Figure 5.

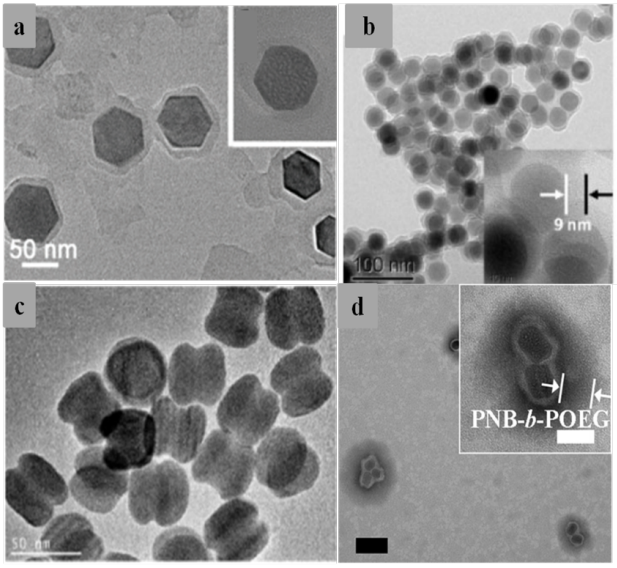

Figure 5: a) TEM images of $NaYF_4$:Yb/Er@PPy core–shell nanoplates. b) $NaYF_4$: Yb/Er@PDA. c) $NaYF_4$:Yb/Er@$NaGdF_4$@ PEG–PAA. d) and diblock copolymer grafted UCNP(UCNP@PNB-b-POEG). Respectively [47, 61–63].

3.3 Silica coating method

UCNPs can be coated by silicon oxidition by covalent bonding of silane hydrolysis. Zhang [21] reported UCNPs compounds (combined with dyes and quantum dots) wrapped with silica by using the silica-coated method, as shown Figure 6. The functional compounds can be issued in different colors of light and widely used in biological probes.

The silica coating method not only can use reverse microemulsion to encapsulate hydrophobic oil-soluble nanoparticles, but also can use microemulsion to encapsulate hydrophilic water-soluble. The encapsulated nanoparticles with good water solubility and biocompatibility are widely used in biomedical fields [64] by silica coating method. Qian [65] prepared mesoporous silica-coated UCNP by microemulsion method. First $NaYF_4$ type UCNPs are coated with TEOS (Figure 7), subsequently,

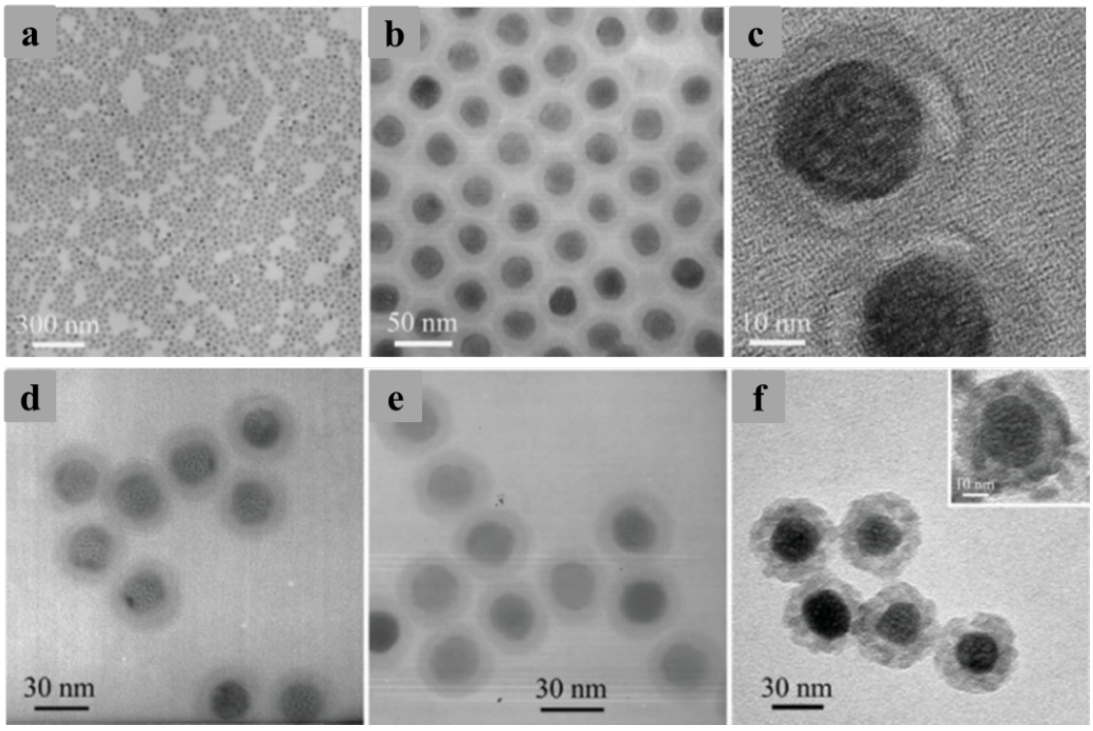

Figure 6: a–c) TEM images of silica-coated $NaYF_4$:Yb,Er nanospheres at different magnifications. TEM images of d) FITC doped silica/$NaYF_4$:Yb,Tm nanospheres, e) TRITC-doped silica/$NaYF_4$:Yb,Er nanospheres, and f) QD605-doped silica/$NaYF_4$:Yb,Tm nanospheres [21].

the mesoporous layer is formed by treating the silica layer with a mixture of TEOS and octadecyltrimethoxysilane (C18TMS). The coated particles are calcined at 500°C to remove excess C18TMS to obtain a mesoporous layer. Then, the photosensitizer zinc phthalocyanine is incorporated into mesoporous layer. Upconversion emission activates the photosensitizer to release singlet oxygen which may kill the cancer cells. Wang *et al.* [66] first prepared a $NaYF_4$:Yb,Er type silica-coated UCNPs by stoy method, then the surface was modified with aminopropyltriethoxysilane amino groups. In silica coating method, neutral polymer can be used to stabilize the silica shell and control its thickness. Wang *et al.* [67] have synthesized UCNPs@SiO_2 with good dispersivity and uniform size by using neutral poly vinylpyrrolidone as stabilizer. Recently Wang *et al.* [68] prepared UCNPs covered with a thin thickness of silica layer by using cetyltrimethylammonium bromide(CTAB) as a template via sol-gel approach. The UCNPs@mSiO_2 surface containing CTAB can be further modified by grafting PAA to form a multifunctional nanocomposite for oral drug delivery.

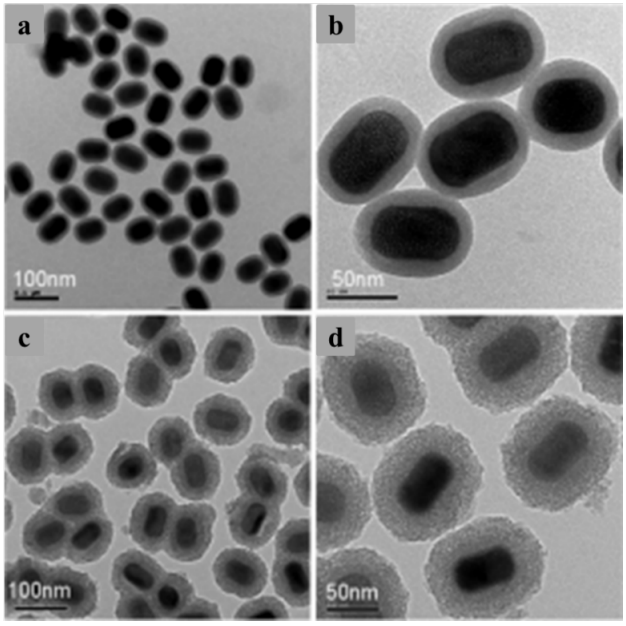

Figure 7: a,b) TEM images of $NaYF_4$:Yb/Er@silica nanoparticles. c,d) mesoporous-silica-coated $NaYF_4$:Yb/Er@silica nanoparticles [65].

3.4 UCNPs@MOF

Besides above mentioned modification methods, the metal-organic frameworks (MOFs) material can also be used for the coating of UCNPs. MOFs are a class of crystalline nanoporous materials with well-defined pore structures [69]. Their unique properties such as high surface area and structural flexibility have endowed them a wide bio-application, ranging from sensors, drug delivery to bioimaging [70, 71]. Sumanta [72] prepared $NaYF_4$:Yb^{3+},Er^{3+}@ZIF-8/FA-5-FU for targeting, imaging and pH responsive drug, ZIF-8 played the role of the drug carrier, as show Figure 8a. Yang [58] also reported that $NaGdF_4$:Yb,Tm@$NaGdF_4$-g-C_3N_4-CDs@ZIF-8 is a multifunctional theranostic for dual-modal photodynamic synergistic therapy via stepwise water splitting, ZIF-8 played the biocompatible role, as shown in figure 8b. Due to ZIF-8 excellent performance, such as high surface area, open metal sites, excellent water stability and biocompatibility, ZIF-8 has become a research hotspot in biomedical materials. Li [73] synthesized core-shell $NaYF_4$:Yb,Tm@MIL-53(Fe)NPs for NIR-enhanced photocatalysis. Liu [74] group also reported that $NaYF_4$:Yb,Er@Fe-MIL-101_NH_2@PEG can be synthesized successfully for luminescent/magnetic dual-mode targeted imaging, as shown Figure 8 c,d. Fe-MOF protects the UCNPs from being quenched for better bioimaging.

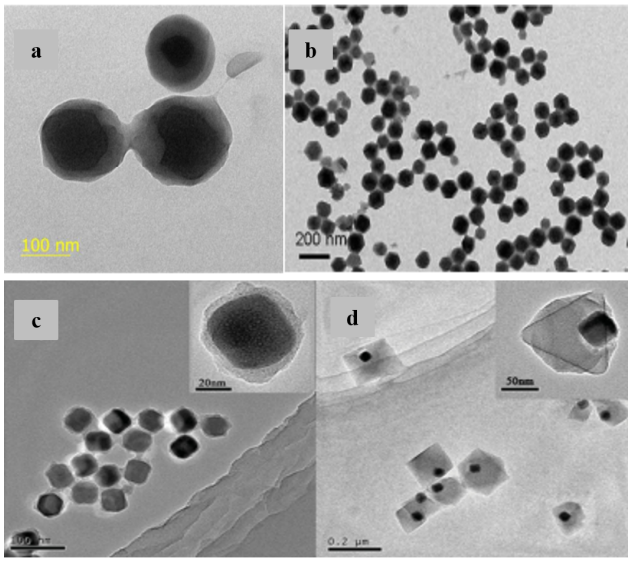

Figure 8: a) HRTEM image of $NaYF_4$: Yb^{3+}, Er^{3+}@ZIF-8. b)TEM image of UCNPs-g-C_3N_4-CDs@ZIF-8. c) UCNP@Fe-MIL-101_NH_2 intermediate products with thin MOF shells, and d) final products with eccentric cores and octahedral MOF shells [58, 72, 74].

4 Biological application of upconversion luminescent nanoparticles

Due to more special advantages over organic dyes and quantum dots, UCNPs have raised to be the most interesting candidate in biological field [40, 46–48, 51, 73, 74]. In recent years, with the development of nanotechnology and biotechnology, upconversion luminescent nanomaterials have been widely used in biomedicine, mainly in the following aspects:

4.1 Biological imaging

Because of few background fluorescence interference, UCNPs have high imaging sensitivity. Li [74] and his colleagues reported synthesis of $NaYF_4$:Yb,Er@MIL-101_NH_2 with 100 nm diameter. The amino group on the surface of $NaYF_4$:Yb,Er@MIL-101_NH_2, is modified by poly(ethylene glycol)-2-amino ethyl ether acetic acid (NH_2-PEG-COOH) and folic acid (FA), resulting in PEGylated UCNP@Fe-MIL-101_NH_2@PEG-FA nanostructures (UMP-FA) and injected them into the diseased mice via the tail vein. There are clear biological imaging by 980nm excitation light irradiation which is shown in Figure 9. $NaYF_4$:Yb,Er@MIL-101_NH_2 mainly accumulates in the liver and there is no other interference of background fluorescence, which

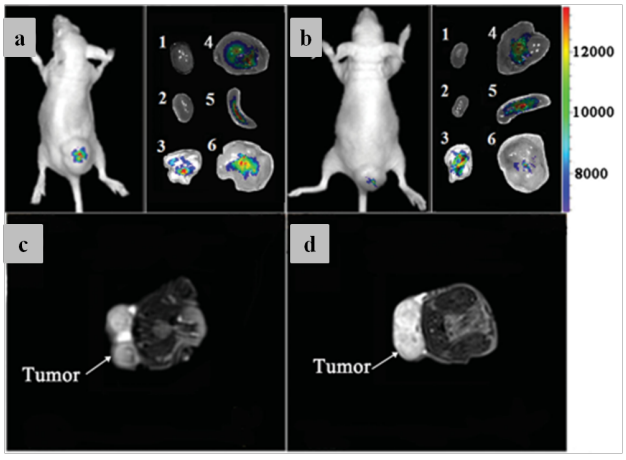

Figure 9: Dual-modal UCL/MR in vivo imaging. Representative UCL imaging of subcutaneous KB tumor-bearing mice and dissected organs of the mice sacrifi ced 24 h after intravenous injection of a) UMP-FAs and b) UMPs. 1, heart;2, kidney; 3, lung; 4, liver; 5, spleen; 6, KB tumor.; Representative T_2-MRI image of KB tumor-bearing mice 24 h after intravenous injection of c) targeted and d) nontargeted UMPs [74].

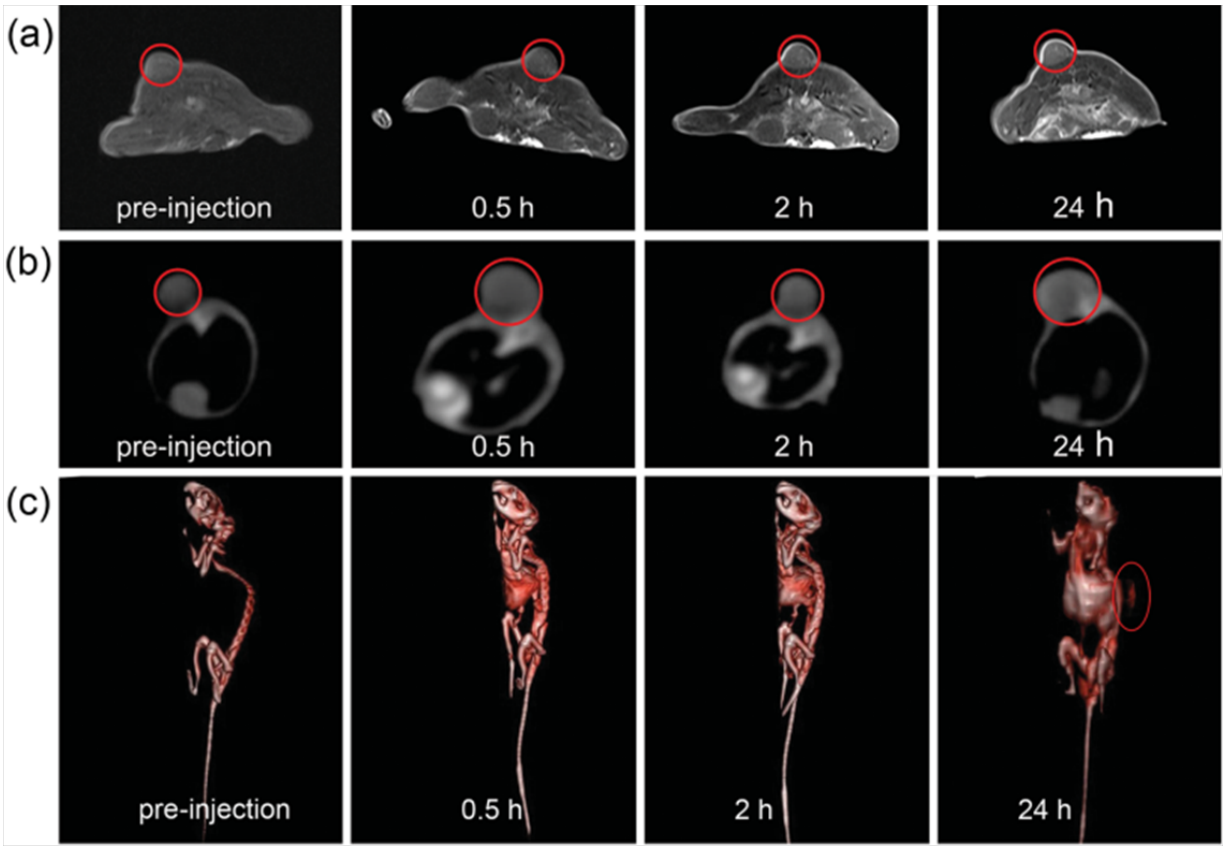

Figure 10: In vivo a) MR and b) CT images c) 3D volume rendering CT images of nude mice after intravenous injection of UCNP@PDA_5-PEG at different timed intervals (pre-injection, 0.5, 2, and 24 h post-injection), respectively. The tumor site was marked by red circle [75].

clearly exhibit the advantages of UCNPs on biological imaging. Wen [62] studied $NaYF_4$:Yb/Er@$NaGdF_4$ for dual-modality fluorescence and magnetic resonance imaging. The element Gd as a protective layer enhanced UCNPs fluorescence intensity, and also as an contrast agent was used for magnetic resonance imaging. Liu [59] synthesized $NaDyF_4$:Yb@$NaLuF_4$:Yb and $NaYF_4$:Yb/Er-Mn for biological imaging. Mn^{2+}-based contrast agents can be used as T_1-weighted MRI probes for visualizing delivery of cancer therapeutic drugs.

UCNPs can be used to integrate a variety of imaging or therapeutic functions through surface modification, making them promising multifunctional nanoplatforms for diagnosis and treatment. For the first time, Wang's group [75] directly covered the near-infrared absorbing polymer PDA on UCNPs, and successfully constructed a multi-functional treatment system UCNP @ PDA_5-PEG-DOX, which can simultaneously achieve up-conversion luminescence (UCL) imaging, T1-weighted magnetic resonance imaging (MRI), X-ray computed tomography (CT) imaging, photothermal therapy (PTT), chemotherapy. PDA not only shows a good photothermal effect, but also can be used as a drug carrier for chemotherapy. Figure 10 shows the in vivo MR, whole-body CT images and 3D volume rendering CT images of nude mice after intravenous injection of UCNP@PDA_5-PEG at different timed intervals, we find that the signal is significantly enhanced over time. These These results have demonstrated that the UCNP@PDA_5-PEG can be employed as contrast agents for in vivo UCL/MRI/CT imaging. Liu and colleagues [76] developed a binary contrast agent based on PAA modified $BaYbF_5$:Tm nanoparticles for direct visualization of the gastrointestinal (GI) tract, displaying low cytotoxicity and negligible hemolysis. Unlike clinically used barium meal, low concentrations of PAA-$BaYbF_5$:Tm can be performed for X-ray imaging of the digestive tract and exhibiting admirable solubility and monodispersity, which greatly reduces the artifacts in the imaging process greatly improve the imaging effect. The in vivo X-ray CT contrast potency of PAA-UCNP was significantly enhanced relative to meglumine pantothenate. Moreover, blood biochemistry assay unambiguously reveal their overall safety and great potentials in biomedicine. Xu and co-workers [77] integrated $NaGdF_4$ doped UCNPs with the Mn-doped silica shell. The

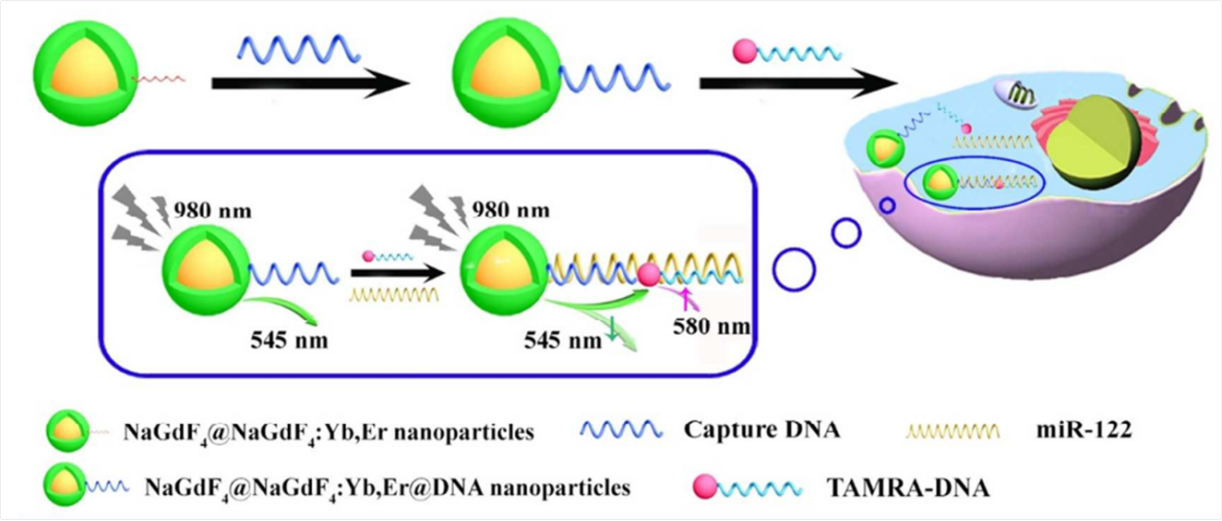

Figure 11: Schematic illustration of the synthesis and workflow of $NaGdF_4$@$NaGdF_4$:Yb,Er@DNA nanoparticles for sensitive detection of miR-122 [80].

Mn-doped silica shell is sensitive to intratumoral acidity and reducibility, causing biodegradation of the shell and further accelerating Si-O-Si bond rupture. Mn release causes MRI effect and Gd^{3+} / Yb^{3+} / Nd^{3+}/ Er^{3+} co-doped UCNP MRI / CT / UCL imaging under 808 nm laser excitation confers multiple imaging capabilities to nanosystems, thereby achieving imaging-guided cancer treatment.

Biologists study intracellular dynamic behavior or nanoscale proteins through a lossless, real-time imaging optical microscope. Due to the existence of optical diffraction limits, conventional far-field optical microscopy cannot observe these life activities at the 200 nm scale. In recent years, super-resolution imaging technology that overcomes the optical diffraction limit has developed rapidly. Currently, UCNPs have been successfully applied to super-resolution microscopy due to significant light penetration depth, ultra-low autofluorescence background and minimal phototoxicity. Jin [78] reported that Yb/Tm co-doped UCNPs are excited by near-infrared light, and blue fluorescence emission can be suppressed. They use this property to design a low-power super-resolution stimulated emission depletion (STED) microscope and realize nanoscale optics. The resolution is 28 nm, which is 1/36 of the wavelength. Recently, Jin [79] introduced that the new near-infrared emission saturation (NIRES) nanodetection mode for deep tissue super-resolution imaging can achieve the same level of imaging resolution (<50 nm) by using simple settings. In the imaging of 93 μm thick liver tissue, they achieved sub-50nm resolution, 1/20th of the excitation wavelength by using 980 nm excitation and detecting at 800 nm. In addition to the above findings, many research teams are now working on UCNPs bioimaging.

4.2 Biological detection

In recent years, chemical biosensors based on the Förster Resonance Energy Transfer (FRET) have been widely used in biomedical and other fields. FRET means when the fluorescence spectrum of one fluorescent molecule (donor) overlaps with the excitation spectrum of another fluorescent molecule (acceptor), donor fluorescent molecule can induce the fluorescence of acceptor, the fluorescence intensity of the acceptor increases with the donor fluorescent molecule itself decaying. The emission wavelength of UCNPs can be controlled by adjusting the elements species and doping ratio. UCNPs are used as energy donors and match energy acceptors to achieve the target detection by FRET. UCNPs can be coupled with DNA, Au nanoparticles, organic dyes, carbon nanoparticles, polyphenylene diamine polymer (PMPD) and other groups. When the groups are coupled, the FRET between them can be achieved and a high sensitive chemical sensor can be designed for bimoleculars detection. As shown in Figure 11, Ren [80] group reported sandwich-DNA-Hybridization FRET strategy for miR-122 detection. Capture DNA-functionalized UCNPs can be regard as energy donor, another short DNA strand labeled with dye of N,N,N',N'-tetramethyl-6-carboxyrhodamine(TAMRA) can be used as energy acceptor, because of the corresponding of UCNPs and TAMRA at 545nm. When miR-122 hybridizes with two above DNA strands, UCNPs and TAMRA can close to each other, resulting the FRET from UCNPs to TAMRA. With the miR-122 concentration increasing, the signal at 545 nm weakens, and the peak at 580 nm strengthens. The changes of the signals can be used as the detection for

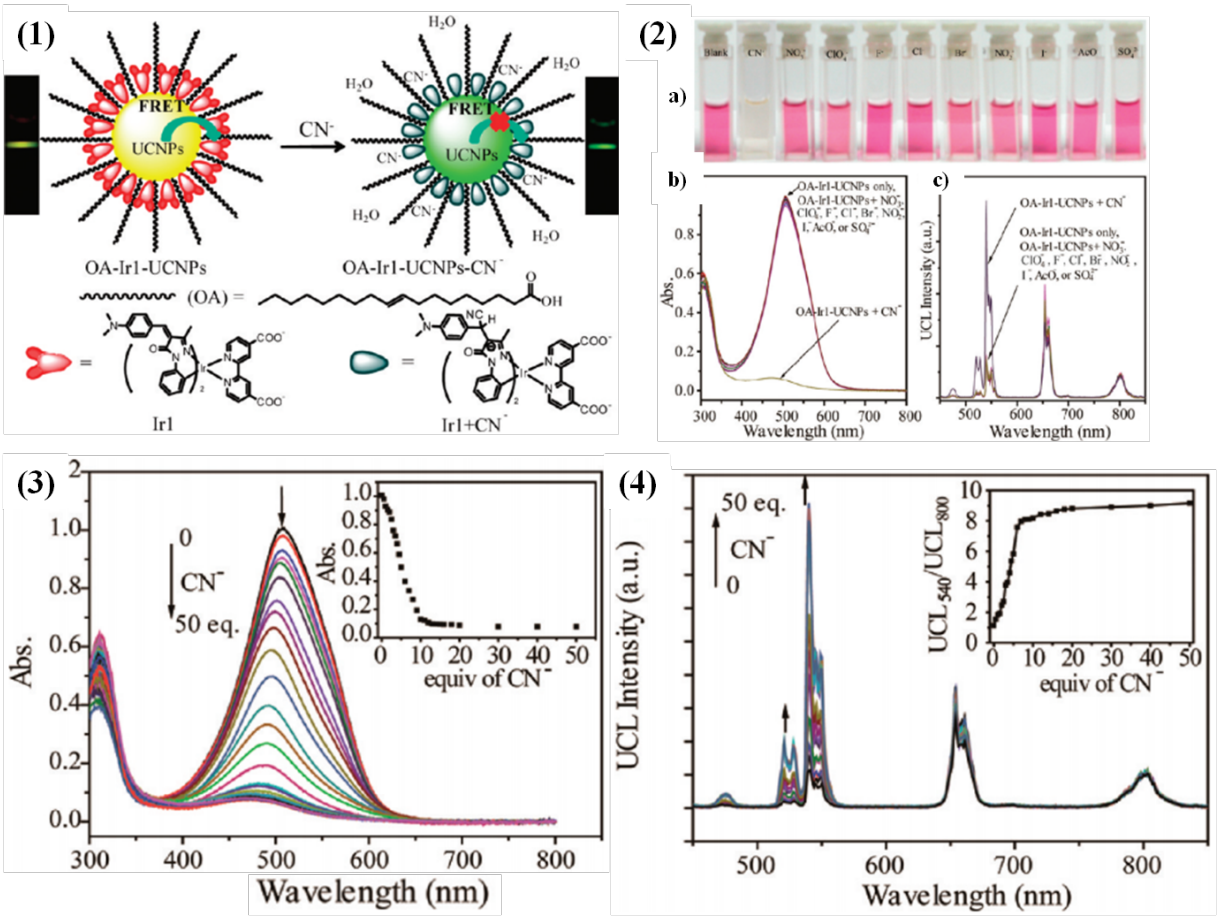

Figure 12: (1) Proposed Recognition Mechanism and the FRET Process of OA-Ir1-UCNPs towards CN^-. (2) The photos of color changes a) of the OA-Ir1-UCNPs upon addition of various anions, and absorption spectra b) and UCL spectra c) of OA-Ir1-UCNPs in DMF/H_2O solution upon addition of 1mM of different anions. Changes in absorption spectra (3) and UCL spectra (4) of 10μM OA-Ir1-UCNPs in DMF/H_2O upon addition of CN. Inset: the absorbance at 505 nm (3) and the ratio (I540/I800) of UCL intensities at 540 and 800 nm (4) of OA-Ir1-UCNPs as a function of CN^- concentration. Excitation by CW 980 nm laser with a power density of 45 W cm^{-2} [82].

miR-22. Sun's group [81] combined a novel Nile red derivative (NRD) with mPEG-modified UCNP to prepare Fe^{3+}-responsive upconversion luminescence nanostructures, which can be used for Fe^{3+} detection.

Li [82] reported that the hydrophobic iridium complex was assembled on the surface of $NaYF_4$:Yb/Er by Van der Waals force (hydrophobic force). At this time, the complex of iridium could effectively absorb the light at 540 nm and result in fluorescence quenching by FRET. Cyanide ions (CN^-) could react with the iridium complex to destroy the iridium conjugate structure, so that the iridium complex lost the absorption ability of 540 nm light. The emission peak at 540 nm of the UCNPs was retained, and the detection of CN^- was achieved by the change of fluorescence intensity at 540nm. The mechanism are shown in Figure 12(1). Figure 12(2) shows colour changes of OA-Ir1-UCNPs solution after adjunction CN^- and other ions at 980nm excitation. The color of sample OA-Ir1-UCNPs+CN^- are colorless, while the others are pink. Absorption peaks of OA-Ir1-UCNPs+CN^- solution at 540 nm are very low and the emission peak is high, which is different from other ions OA-Ir1-UCNPs. The special phenomenon leads to CN^- selective detection characteristic. In addition, the fluorescence quenching degree of the iridium complex at 540 nm was different according to the change of CN^- concentration, so the CN^- concentration detection can be realized, which is shown in Figure 12(3,4).

4.3 New type of cancer photodynamic therapy

Photodynamic therapy refers to the transfer of some drugs (Photosensitive molecules) into tissues under light conditions to absorb photon energy to produce reactive oxygen species (O^{2-}, $^1O_2$), finally result in the destroy of

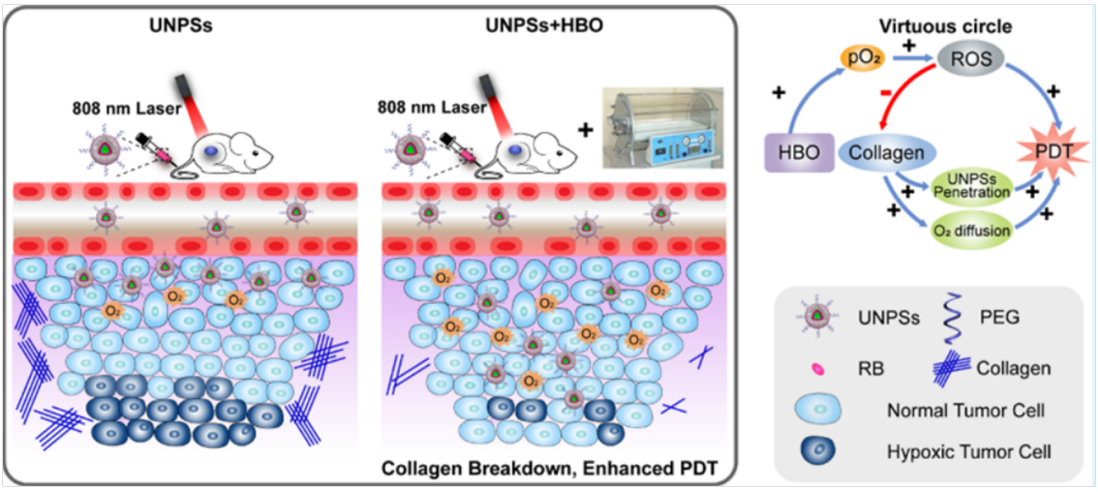

Figure 13: Schematic Illustration of Synergizing UNPSs with or without HBO for Remodelling Collagen in the ECM To Achieve Better Oxygenation and Deeper Penetration of Nano-PSs for Enhanced Photodynamic Cancer Therapy [83].

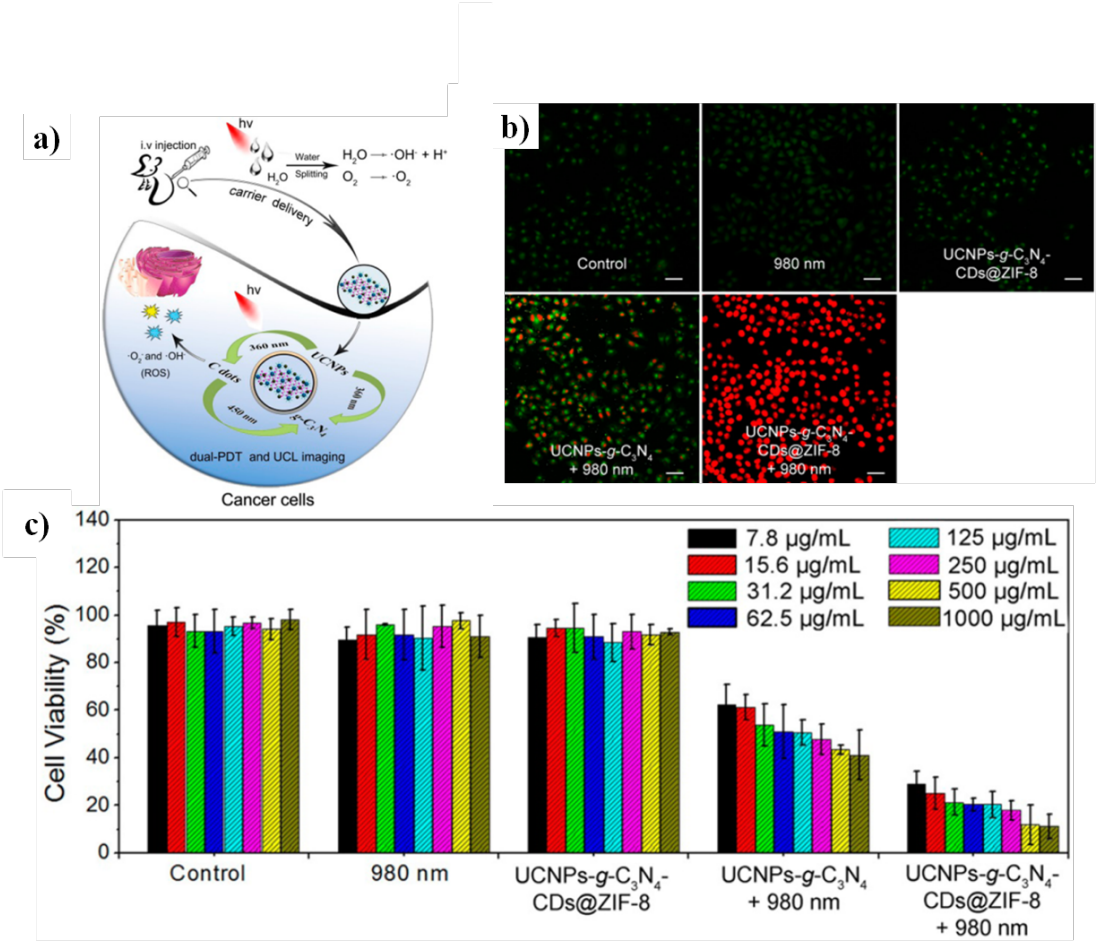

Figure 14: a) Reaction mechanism diagram. b) CLSM images of HeLa cells incubated with different conditions corresponding to the toxicity test in vitro, and all the cells are marked with calcein AM and PI. Scale bars for all images are 50μm. c) In vitro cell viabilities of HeLa cells incubated with cellculture (control), 980nm light, UCNPs-g-C_3N_4 with 980nm laser irradiation and UCNPs-g-C_3N_4-CDs@ ZIF-8 at varied concentrations with and without 98 nm laser irradiation [58].

the nearby tumor cells. The low cost, the minimum side effects, high efficiency and minimal extra trauma [34, 82] are the specific advantages of the method. Zhang group [83] reports hyperbaric oxygen-assisted and upconverted nanophotosensitive agents (UNPSs) to mediate synergistic photodynamic cancer treatment. They effectively solved the problem that hypoxic tumor microenvironment and tumor extracellular matrix (ECM) limit the availability of molecular oxygen and the depth of delivery of photosensitizers (PSs) within tumors. First, the UCNPs with high tissue penetration depth and ROS-generating PSs are combined to synthesize UNPSs, and energy resonance transfer can occur between them. When near-infrared light is excited at 808 nm the HBO-assisted photodynamic process can remodel the tumor microenvironment by breaking down the collagen matrix in the ECM. Even in the hypoxic tumor microenvironment, efficient photodynamic processes can be activated by energy transfer from the upconversion core to the RB, and then sensitized to produce cytotoxic ROS. Schematic diagram is shown in Figure 13.

Yang [58] and his colleagues synthesized a two-photodynamic therapy system by using two photosensitizer molecules g-C_3N_4 and CDs which could absorb light by UCNPs emitted at 980nm excitation. The two-photodynamic therapy system could decompose oxygen in the tissue to produce reactive oxygen to kill cancer cells. It overcomes the shortcomings of the UV tissue penetration depth and achieve the maximum use of light energy. Mechanism as shown in Figure 14a. Figure 14b,c show that the therapeutic effect of UCNPs-g-C_3N_4-CDs@ZIF-8 at 980 nm laser on cancer is better than that of the control. Figure 13c shows that UCNPs-g-C_3N_4-CDs@ZIF-8 composite has no significant difference compared with the control group, high cell viability can be more than 80%.

Because of nontoxic, good biocompatibility, excellent biological imaging ability and effective cancer treatment, many research groups have conducted research on photodynamic therapy based on various upconversion luminescent nanoparticles, such as $NaDyF_4$:Yb @ :Yb/Er@Polydopamine [59], $NaYF_4$:Yb/Er @ PPy [47], $NaYF_4$:Yb/Er @ $NaYF_4$:Yb @ $NaNdF_4$:Yb [84], mesoporous-silica-coated UCNPs [65] etc. The new type of cancer photodynamic therapy displays a very large application prospect.

5 Summary

In this study, the luminescence mechanism, preparation method, surface modification of upconversion fluorescent nanoparticles and application in biomedical field are discussed. By controlling experimental conditions, the shape of the particles can be topographically controlled, and the size is usually uniform. The excellent properties of UCNPs series overcome the shortcomings of low penetrability, destructive biological tissue and interference of autofluorescence of fluorescent dyes and quantum dots, and UCNPs have been widely used in the field of biomedicine. As the reports about UCNPs increasing year by year, UCNPs undoubtedly can replace the traditional fluorescent materials, while there is still a large gap for clinical applications. In order to better application of UCNPs in the biomedical field, high photosensitized upconversion nanoparticle with smaller size, higher loading rate and more tunable color performance is still a challenge. Designing low-biotoxic, multiphoton excited near-infrared fluorescent probes, with significantly high bioimaging resolution and high imaging depth, is an important direction for the development of biomedical fluorescent probes. In the near future, with the rapid development of upconversion luminescent nanoparticles, coupled with scientific and technological improvements, making the UCNPs technology become a universal solution to solve many of today's challenging medical problems maybe possible.

Acknowledgement: F. J. and G. L. contributed equally to this work. This work is financially supported by General Financial Grant from China Postdoctoral (2017M612203), the National Natural Science Foundation of China (51804174, 21675091, 21574072, 21874078), the Taishan Young Scholar Program of Shandong Province (tsqn20161027), the Key Research and Development Project of Shandong Province (2016GGX102028, 2016GGX102039, 2017GGX20111), the Natural Science Foundation of Shandong Province (ZR2017BEE010), the Project of Shandong Province Higher Educational Science and Technology Program (J15LC20), the Scientific Research Foundation for the Returned Overseas Chinese Scholars of State Education Ministry (20111568), the People's Livelihood Science and Technology Project of Qingdao (166257nsh, 173378nsh), the Innovation Leader Project of Qingdao (168325zhc), the Postdoctoral Scientific Research Foundation of China (40617010030), The Major Science and Technology Innovation Project of Shandong Province (2018CXGC1407), and the First Class Discipline Project of Shandong Province.

Author Contributions: All the authors described and wrote in the attached files.

Conflict of Interests: The authors declare no conflict of interest.

References

[1] Sun L, Wei R, Feng J, Zhang H. Tailored lanthanide-doped upconversion nanoparticles and their promising bioapplication prospects. Coord. Chem. Rev. 2018, 364, 10-32.

[2] He F, Niu N, Wang L, Xu J, Wang Y, Yang G, Gai S, Yang P. Influence of surfactants on the morphology, upconversion emission, and magnetic properties of beta- $NaGdF_4$:Yb^{3+},Ln^{3+} (Ln = Er, Tm, Ho). Dalton T 2013, 42, 10019-10028.

[3] Chen D, Wan Z, Zhou Y, Huang P, Zhong J, Ding M, Xiang W, Liang X, Ji Z. Bulk glass ceramics containing Yb^{3+}/Er^{3+}: β-$NaGdF_4$ nanocrystals: Phase-separation-controlled crystallization, optical spectroscopy and upconverted temperature sensing behavior. J Alloy Compd 2015, 638, 21-28.

[4] Bloembergen N. Solid state infrared quantum counters. Phys Rev Lett 1959, 2, 84-85.

[5] Labbe C, Dounlan JL, Camy P, Moncorge R, Thuau M. The 2:8 µm laser properties of Er^{3+} doped CaF_2 crystals. Opt Commun 2002, 209, 193–199.

[6] Wang F, Deng R, Wang J, Wang Q, Han Y, Zhu H, Chen X, Liu X. Tuning upconversion through energy migration in core-shell nanoparticles. Nature materials 2011, 10, 968-973.

[7] Mader HS, Kele P, Saleh SM, Wolfbeis OS. Upconverting luminescent nanoparticles for use in bioconjugation and bioimaging. Curr Opin Chem Biol 2010, 14, 582-596.

[8] Thao CTB, Huy BT, Sharipov M, Kim JI, Dao VD, Moon JY, Lee YI. Yb^{3+},Er^{3+},Eu^{3+}-codoped YVO_4 material for bioimaging with dual mode excitation. Mat Sci Eng C-Mater 2017, 75, 990-997.

[9] Qiu H, Tan M, Ohulchanskyy T, Lovell J, Chen G. Recent progress in upconversion photodynamic therapy. Nanomaterials 2018, 8, 344.

[10] Haase M, Schafer H. Upconverting nanoparticles. Angew Chem Int Edit 2011, 50, 5808-5829.

[11] Wang F, Han Y, Lim CS, Lu YH, Wang J, Xu J, Chen HY, Zhang C, Hong MH, Liu XG. Simultaneous phase and size control of upconversion nanocrystals through lanthanide doping. Nature 2010, 463, 1061-1065.

[12] Deng R, Xie X, Vendrell M, Chang YT, Liu X. Intracellular glutathione detection using mno(2)-nanosheet-modified upconversion nanoparticles. J Am Chem Soc 2011, 133, 20168-20171.

[13] Liu Y, Zhou S, Tu D, Chen Z, Huang M, Zhu H, Ma E, Chen X. Amine-functionalized lanthanide-doped zirconia nanoparticles: Optical spectroscopy, time-resolved fluorescence resonance energy transfer biodetection, and targeted imaging. J Am Chem Soc 2012, 134, 15083-15090.

[14] He M, Huang P, Zhang C, Hu H, Bao C, Gao G, He R, Cui D. Dual phase-controlled synthesis of uniform lanthanide-doped $NaGdF_4$ upconversion nanocrystals via an oa/ionic liquid two-phase system for in vivo dual-modality imaging. Adv Func Mater 2011, 21, 4470-4477.

[15] Chen D, Liu L, Huang P, Ding M, Zhong J, Ji Z. Nd(3+)-sensitized Ho(3+) single-band red upconversion luminescence in core-shell nanoarchitecture. J Phys Chem Lett 2015, 6, 2833-2840.

[16] Chen S, Weitemier AZ, Zeng X, He LM, Wang XY, Tao YQ, Huang AJY, Yuki Hashimotodani Y, Kano M, Iwasaki H, Parajuli LK, Okabe S et al. Near-infrared deep brain stimulation via upconversion nanoparticle–mediated optogenetics. Science 2018, 359, 679-684.

[17] Li H, Wei R, Yan GH, Sun J, Li C, Wang H, Shi L, Capobianco JA, Sun L. Smart self-assembled nanosystem based on water-soluble pillararene and rare-earth-doped upconversion nanoparticles for ph-responsive drug delivery. ACS Appl. Mater. Interfaces 2018, 10, 4910-4920.

[18] Yi GS, Lu HC, Zhao SY, Yue G, Yang WJ, Chen DP, Guo LH. Synthesis, characterization, and biological application of size-controlled nanocrystalline NaYF4 : Yb,Er infrared-to-visible upconversion phosphors. Nano Lett 2004, 4, 2191-2196.

[19] Heer S, Kompe K, Gudel HU, Haase M. Highly efficient multicolour upconversion emission in transparent colloids of lanthanide-doped $NaYF_4$ nanocrystals. Adv Mater 2004, 16, 2102-2105.

[20] Lu Q, Hou Y, Tang A, Lu Y, Lv L, Teng F. Controlled synthesis and defect dependent upconversion luminescence of Y_2O_3: Yb, Er nanoparticles. J Appl Phys 2014, 115, 074309.

[21] Li Z, Zhang Y, Jiang S. Multicolor core/shell-structured upconversion fluorescent nanoparticles. Adv Mater 2008, 20, 4765-4769

[22] Qiu HL, Yang CH, Shao W, Damasco J, Wang XL, Ågren H, Prasad PN. Guanying Chen, G.Y. Enhanced Upconversion Luminescence in Yb^{3+}/Tm^{3+}-Codoped Fluoride Active Core/Active Shell/Inert Shell Nanoparticles through Directed Energy Migration. Nanomaterials 2014, 4, 55-68.

[23] Boyer JC, Vetrone F, Cuccia LA, Capobianco JA. Synthesis of colloidal upconverting $NaYF_4$ nanocrystals doped with Er^{3+}, Yb^{3+} and Tm^{3+}, Yb^{3+} via thermal decomposition of lanthanide trifluoroacetate precursors. J Am Chem Soc 2006, 128, 7444-7445.

[24] Boyer JC, Cuccia LA, Capobianco JA. Synthesis of colloidal upconverting $NaYF_4$: Er^{3+}/Yb^{3+} and Tm^{3+}/Yb^{3+} monodisperse nanocrystals. Nano Lett 2007, 7, 847-852.

[25] Mahalingam V, Vetrone F, Naccache R, Speghini A, Capobianco JA. Colloidal Tm^{3+}/Yb^{3+}-doped $LiYF_4$ nanocrystals: Multiple luminescence spanning the uv to nir regions via low-energy excitation. Adv Mater 2009, 21, 4025-+.

[26] Mahalingam V, Naccache R, Vetrone F, Capobianco JA. Sensitized Ce^{3+} and Gd^{3+} ultraviolet emissions by Tm^{3+}in colloidal $LiYF_4$ nanocrystals. Chem-Eur J 2009, 15, 9660-9663.

[27] Vetrone F, Naccache R, Mahalingam V, Morgan CG, Capobianco JA. The active-core/active-shell approach: A strategy to enhance the upconversion luminescence in lanthanide-doped nanoparticles. Adv Funct Mater 2009, 19, 2924-2929.

[28] Kang N, Liu Y, Zhou YM, Wang D, Chen C, Ye SF, Nie LM, Ren L. Phase and size control of core-shell upconversion nanocrystals light up deep dual luminescence imaging and ct in vivo. Adv Healthc Mater 2016, 5, 1356-1363.

[29] Wang F, Deng R, Liu X. Preparation of core-shell $NaGdF_4$ nanoparticles doped with luminescent lanthanide ions to be used as upconversion-based probes. Nature Protocols 2014, 9, 1634-1644.

[30] Li H, Xu L, Chen G. Controlled synthesis of monodisperse hexagonal $NaYF_4$:Yb/Er nanocrystals with ultrasmall size and enhanced upconversion luminescence. Molecules 2017, 22, 2113.

[31] Chen DQ, Yu YL, Huang F, Huang P, Yang AP, Wang YS. Modifying the size and shape of monodisperse bifunctional alkaline-earth fluoride nanocrystals through lanthanide doping. J Am Chem Soc 2010, 132, 9976-9978.

[32] Yi MJ, Liu YF, Gao HP, Huang ZY, Liang JW, Mao YL. Upconversion effective enhancement of $NaYF_4$:Yb^{3+}/Er^{3+} nanoparticles by Ni^{2+} doping. J Mater Sci 2018, 53, 1395-1403.

[33] Xu HY, Prasad M, He XL, Shan LW, Qi SY. Discoloration of rhodamine b dyeing wastewater by schorl-catalyzed fenton-like reaction. Sci China Ser E 2009, 52, 3054-3060.

[34] Dou JT, Hou YB. Upconversion luminescence of ZBLAN:Yb^{3+}, Tm^{3+} co-excited by double-frequency with both 808 and 980 nm lasers. Chin J Lumin 2008; 29, 85-88.

[35] Hua R, Zang CY, Shao C, Xie D, Shi CS. Synthesis of barium fluoride nanoparticles from microemulsion. Nanotechnology 2003,14,588—591

[36] Hua R, Lei BF, Xie D, Shi CS. Synthesis of Calcium Fluoride Nanoparticles from Microemulsion. Chin. J. Chin. Univ 2003, 24, 1756-1764.

[37] Luo XX, Cao WH. Ethanol-assistant solution combustion method to prepare la2o2s:Yb,pr nanometer phosphor. J Alloy Compd 2008, 460, 529-534.

[38] Xu L, Yu Y, Li X, Somesfalean G, Zhang Y, Gao H. Zhang Z. Synthesis and upconversion properties of monoclinic gd2o3:Er3+ nanocrystals. Opt Mater 2008, 30, 1284-1288.

[39] Vetrone F, Boyer JC, Capobianco JA, Speghini A, Bettinelli M. Significance of Yb^{3+}concentration on the upconversion mechanisms in codoped Y_2O_3:Er^{3+}, Yb^{3+} nanocrystals. J Appl Phys 2004, 96, 661-667.

[40] Liu C, Wang H, Li X, Chen D. Monodisperse, size-tunable and highly efficient β-$NaYF_4$:Yb,Er(Tm) up-conversion luminescent nanospheres: Controllable synthesis and their surface modifications. J Mater Chem 2009, 19, 3546-3553.

[41] Wang L, Zhang Y, Zhu Y. One-pot synthesis and strong near-infrared upconversion luminescence of poly(acrylic acid)-functionalized YF_3:Yb^{3+}/Er^{3+} nanocrystals. Nano Research 2010, 3, 317-325.

[42] Biju S, Gallo J, Banobre-Lopez M, Manshian BB, Soenen SJ, Himmelreich U, Vander Elst L, Parac-Vogt TN. A magnetic chameleon: Biocompatible lanthanide fluoride nanoparticles with magnetic field dependent tunable contrast properties as a versatile contrast agent for low to ultrahigh field mri and optical imaging in biological window. Chem-Eur J 2018, 24, 7388-7397.

[43] Ai XZ, Lyu LN, Mu J, Hu M, Wang ZM, Xing BG. Synthesis of core-shell lanthanide-doped upconversion nanocrystals for cellular applications. J Vis Exp 2017, 129, 1-9.

[44] Boyer JC, Manseau MP, Murray JI., van Veggel FC. Surface modification of upconverting $NaYF_4$ nanoparticles with peg-phosphate ligands for NIR (800 nm) biolabeling within the biological window. Langmuir 2010, 26, 1157-1164

[45] Wang BY, Liao ML, Hong GC, Chang WW, Chu CC. Near-infrared-triggered photodynamic therapy toward breast cancer cells using dendrimer-functionalized upconversion nanoparticles. Nanomaterials 2017, 7, 1-18.

[46] Wang C, Cheng L, Liu Z. Drug delivery with upconversion nanoparticles for multi-functional targeted cancer cell imaging and therapy. Biomaterials 2011, 32, 1110-1120.

[47] Huang X, Li B, Peng C, Song G, Peng Y, Xiao Z, Liu X, Yang J, Yu L, Hu J. $NaYF_4$:Yb/Er@PPy core-shell nanoplates: an imaging-guided multimodal platform for photothermal therapy of cancers. Nanoscale 2016, 8, 1040-1048.

[48] Xiao Q, Li Y, Li F, Zhang M, Zhang Z, Lin H. Rational design of a thermalresponsive-polymer-switchable fret system for enhancing the temperature sensitivity of upconversion nanophosphors. Nanoscale 2014, 6, 10179-10186.

[49] Li Y, Tang J, He L, Liu Y, Liu Y, Chen C, Tang Z. Core-shell upconversion nanoparticle@metal-organic framework nanoprobes for luminescent/magnetic dual-mode targeted imaging. Adv Mater 2015, 27, 4075-4080.

[50] Li M, Zheng Z, Zheng Y, Cui C, Li C, Li Z. Controlled growth of metal-organic framework on upconversion nanocrystals for nir-enhanced photocatalysis. Acs Appl Mater Inter 2017, 9, 2899-2905.

[51] Xing Y, Li L, Ai X, Fu L. Polyaniline-coated upconversion nanoparticles with upconverting luminescent and photothermal conversion properties for photothermal cancer therapy. Int J Nanomed 2016, 11, 4327-4338.

[52] Yi GS, Chow GM. Water-Soluble $NaYF_4$:Yb,Er(Tm)/$NaYF_4$/Polymer Core/Shell/Shell Nanoparticles with Significant Enhancement of Upconversion Fluorescence. Chem Mater 2007, 19, 341-343.

[53] Kim WJ, Nyk M, Prasad PN. Color-coded multilayer photopatterned microstructures using lanthanide (iii) ion co-doped $NaYF_4$ nanoparticles with upconversion luminescence for possible applications in security. Nanotechnology 2009, 20, 185301.

[54] Kamimura M, Miyamoto D, Saito Y, Soga K, Nagasaki Y. Design of poly(ethylene glycol)/streptavidin coimmobilized upconversion nanophosphors and their application to fluorescence biolabeling. Langmuir 2008, 24, 8864-8870.

[55] Hilderbrand SA, Shao FW, Salthouse C, Mahmood U, Weissleder R. Upconverting luminescent nanomaterials: Application to in vivo bioimaging. Chem Commun 2009, 4188-4190.

[56] Chatterjee DK, Rufaihah AJ, Zhang Y. Upconversion fluorescence imaging of cells and small animals using lanthanide doped nanocrystals. Biomaterials 2008, 29, 937-943.

[57] Wang F, Chatterjee DK, Li ZQ, Zhang Y, Fan XP, Wang MQ. Synthesis of polyethylenimine/$NaYF_4$ nanoparticles with upconversion fluorescence. Nanotechnology 2006, 17, 5786-5791.

[58] Yang D, Yang G, Gai S, He F, Li C, Yang P. Multifunctional theranostics for dual-modal photodynamic synergistic therapy via stepwise water splitting. ACS. Appl Mater Inter 2017, 9, 6829-6838.

[59] Liu T, Li S, Liu Y, Guo Q, Wang L, Liu D, Zhou J. Mn-complex modified $NaDyF_4$:Yb@$NaLuF_4$:Yb,Er@polydopamine core–shell nanocomposites for multifunctional imaging-guided photothermal therapy. J Mater Chem B 2016, 4, 2697-2705.

[60] Ma L, Liu F, Lei Z, Wang Z. A novel upconversion@polydopamine core@shell nanoparticle based aptameric biosensor for biosensing and imaging of cytochrome c inside living cells. Biosens Bioelectron 2017, 87, 638-645.

[61] Liu Y, Tu D, Zheng W, Lu L, You W, Zhou S, Huang P, Li R, Chen X. A strategy for accurate detection of glucose in human serum and whole blood based on an upconversion nanoparticles-polydopamine nanosystem. Nano Research 2018, 11, 3164-3174.

[62] Wen HQ, Peng HY, Liu K, Bian MH, Xu YJ, Dong L, Yan X, Xu WP, Tao W, Shen JL. Sequential Growth of $NaYF_4$:Yb/Er@$NaGdF_4$Nanodumbbells for Dual-Modality Fluorescence and Magnetic Resonance Imaging. Acs Appl Mater Inter 2017, 9, 9226-9232.

[63] Xiang J, Tong X, Shi F, Yan Q, Yu B, Zhao Y. Near-infrared light-triggered drug release from uv-responsive diblock copolymer-coated upconversion nanoparticles with high monodispersity. J Mater Chem B 2018, 6, 3531-3540.

[64] Dai YL, Ma PA, Cheng ZY, Kang XJ, Zhang X, Hou ZY, Li CX, Yang DM, Zhai XF, Lin J. Up-conversion cell imaging and phinduced thermally controlled drug release from

$NaYF_4$:Yb^{3+}/Er^{3+}@hydrogel core-shell hybrid microspheres. ACS nano 2012, 4, 3327–3338.

[65] Qian HS, Guo HC, Ho PC, Mahendran R, Zhang Y. Mesoporous-silica-coated up-conversion fluorescent nanoparticles for photodynamic therapy. Small 2009, 5, 2285-2290.

[66] Wang M, Hou W, Mi CC, Wang WX, Xu ZR, Teng HH, Mao CB, Xu SK. Immunoassay of goat antihuman immunoglobuling antibody based on luminescence resonance energy transfer between near-infrared responsive $NaYF_4$:Yb, Er upconversion fluorescent nanoparticles and gold nanoparticles. Anal Chem. 2009, 81, 8783–8789.

[67] Li Z, Zhang Y. Monodisperse silica-coated polyvinylpyrrolidone/NaYF(4) nanocrystals with multicolor upconversion fluorescence emission. Angew Chem 2006, 45, 7732-7735.

[68] Liu SH, Tian BS, Wu SY, Wang YB, Huang JB, Gao B, Jin L, Li K, Wang ZL. pH-sensitive polymer-gated multifunctional upconversion NaYF4:Yb/Er@$mSiO_2$ nanocomposite for oral drug delivery. Microporous Mesoporous Mater 2018, 264, 151–158

[69] Furukawa H, Cordova KE, O'Keeffe M, Yaghi OM. The chemistry and applications of metal-organic frameworks. Science 2013, 341, 1230444.

[70] Cui C, Liu Y, Xu H, Li S, Zhang W, Cui P, Huo F. Self-assembled metal-organic frameworks crystals for chemical vapor sensing. Small 2014, 10, 3672-3676.

[71] Murray LJ, Dinca M, Long JR. Hydrogen storage in metal-organic frameworks. Chem Soc Rev 2009, 38, 1294-1314.

[72] Chowdhuri AR, Laha D, Pal S, Karmakar P, Sahu SK. One-pot synthesis of folic acid encapsulated upconversion nanoscale metal organic frameworks for targeting, imaging and ph responsive drug release. Dalton. T. 2016, 45, 18120-18132.

[73] Li MH, Zheng ZJ, Zheng YQ, Cui C, Li CX, Li ZQ. Controlled growth of metal-organic framework on upconversion nanocrystals for nir-enhanced photocatalysis. Acs. Appl. Mater. Inter 2017, 9, 2899-2905.

[74] Li YT, Tang JL, He LC, Liu Y, Liu YL, Chen CY, Tang ZY. Core-shell upconversion nanoparticle@metal-organic framework nanoprobes for luminescent/magnetic dual-mode targeted imaging. Adv. Mater 2015, 27, 4075-4080.

[75] Liu F, He X, Lei Z, Liu L, Zhang J, You H, Zhang H, Wang Z. Facile preparation of doxorubicin-loaded upconversion@polydopamine nanoplatforms for simultaneous in vivo multimodality imaging and chemophotothermal synergistic therapy. Adv Healthc Mater 2015, 4, 559-568.

[76] Liu Z, Ju E, Liu J, Du Y, Li Z, Yuan Q, Ren J, Qu X. Direct visualization of gastrointestinal tract with lanthanide-doped baybf5 upconversion nanoprobes. Biomaterials 2013, 34, 7444-7452.

[77] Xu JT, Han W, Cheng ZY, Yang PP, Bi HT, Yang D, Niu N, He F, Gai SL, Lin J. Bioresponsive and near infrared photon co-enhanced cancer theranostic based on upconversion nanocapsules. Chem Sci 2018, 9, 3233-3247.

[78] Liu Y, Lu Y, Yang X, Zheng X, Wen S, Wang F, Vidal X, Zhao J, Liu D, Zhou Z. Amplified stimulated emission in upconversion nanoparticles for super-resolution nanoscopy. Nature 2017, 543, 229-233.

[79] Chen C, Wang F, Wen S, Su QP, Wu MCL, Liu Y, Wang B, Li D, Shan X, Kianinia M. Multi-photon near-infrared emission saturation nanoscopy using upconversion nanoparticles. Nature communications 2018, 9, 3290.

[80] Ren H, Long Z, Shen X, Zhang Y, Sun J, Ouyang J, Na N. A sandwich-DNA-hybridization fret strategy for mir-122 detection by core-shell upconversion nanoparticles. Acs. Appl. Mater. Inter 2018, DOI: 10.1021/acsami.8b03429.

[81] Wei R, Wei Z, Sun L, Zhang JZ, Liu J, Ge X, Shi L. Nile red derivative-modified nanostructure for upconversion luminescence sensing and intracellular detection of Fe(3+) and mr imaging. ACS Appl. Mater. Interfaces 2016, 8, 400-410.

[82] Liu J, Liu Y, Liu Q, Li C, Sun L, Li F. Iridium(iii) complex-coated nanosystem for ratiometric upconversion luminescence bioimaging of cyanide anions. J. Am. Chem. Soc 2011, 133, 15276-15279.

[83] Li J, Huang J, Ao Y, Li S, Miao Y, Yu Z, Zhu L, Lan X, Zhu Y, Zhang Y. Synergizing upconversion nanophotosensitizers with hyperbaric oxygen to remodel the extracellular matrix for enhanced photodynamic cancer therapy. ACS. Appl. Mater. Interfaces 2018, 10, 22985–22996.

[84] Peng HY, Ding BB, Ma YC, Sun SQ, Tao W, Guo YC, Guo HC, Yang XZ, Qian HS. Sequential growth of sandwiched NaYF4:Yb/Er@NaYF4:Yb@NaNdF4:Yb core–shell–shell nanoparticles for photodynamic therapy. Appl. Surf. Sci 2015, 357, 2408-2414.